ChemComm

Layer-by-Layer Preparation of Polyelectrolyte Multilayer Nanocapsules via Crystallized Miniemulsions

Journal:	*ChemComm*
Manuscript ID	CC-COM-10-2018-008043.R1
Article Type:	Communication

Journal Name

COMMUNICATION

Layer-by-layer preparation of polyelectrolyte multilayer nanocapsules via crystallized miniemulsions

Received 00th January 20xx,
Accepted 00th January 20xx

DOI: 10.1039/x0xx00000x

www.rsc.org/

Amin Jafari,[a] Haotian Sun,[a] Boyang Sun,[a] Mohamed Alaa Mohamed,[a,b] Honggang Cui,[c] and Chong Cheng[a]*

Well-defined polyelectrolyte multilayer nanocapsules (NCs) are synthesized by layer-by-layer deposition of poly(acrylic acid) and poly(allylamine hydrochloride) over crystallized miniemulsion nanoparticles, followed by shell crosslinking and template removal. This synthetic approach allows well-controlled dimensions of NCs due to the high colloidal stability of the templates, and may also permit a broad composition range of NCs because of the mild conditions for template removal.

Polymeric capsules have attracted significant interests because of their hollowed structures that can be utilized for various applications.[1] The composition and dimensions of polymeric capsules are critically important for tuning their comprehensive properties and targeting specific applications.[2] For instance, nanocapsules (NCs) with biocompatible polymeric components have proven to be a promising class of nanocarriers for applications in the delivery of therapeutic and diagnostic agents via blood circulation.[3]

Among various approaches, layer-by-layer (LBL) self-assembly as a versatile technique has been developed for the synthesis of capsules with well-controlled polyelectrolyte multilayer (PEM) structures.[1a-1c] The corresponding preparation relies on the use of sacrificial cores as substrates for LBL deposition and templates of capsule cavities, which are formed after core removal. Therefore, the size, stability, and removal conditions of such sacrificial cores are critical in the synthetic control of capsules. Accordingly, there are two general synthetic limitations. First, it is more difficult to prepare smaller capsules, because high colloidal stability of LBL cores is required to overcome their aggregation tendency which becomes more severe for smaller templates especially during the LBL depositing and subsequent washing process.[4] Second, the processing conditions for the removal of LBL cores can impose significant restrictions on the composition of polyelectrolyte layers. Emulsion-derived templates, with liquid,[5] liquid crystal,[6] or hydrogel[7] droplets covered by interface-stabilizing substances, have been utilized in LBL preparation of capsules. These templates can allow core removal under mild conditions, and therefore enable a broad range of composition of capsules. However, generally the resulting capsules were limited to micron size, and it is very challenging to prepare well-defined NCs via these templates for several reasons. First, typically emulsion-derived templates have relatively limited colloidal stability due to the dynamic nature of small molecule surfactants. Second, although larger-sized interface-stabilizing substances can lead to emulsions with higher colloidal stability,[8] the sizes of these emulsions are generally in micron range. Third, low polydispersity of emulsion-derived droplets may not be obtained in some systems.

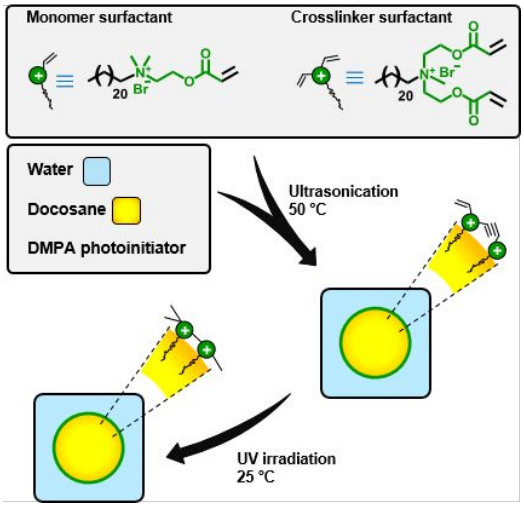

Scheme 1. Preparation of crystallized miniemulsion

[a] Department of Chemical and Biological Engineering, University at Buffalo, The State University of New York, Buffalo, NY 14260, USA. E-mail: ccheng8@buffalo.edu
[b] Chemistry Department, College of Science, Mansoura University, Mansoura, 35516, Egypt
[c] Department of Chemical and Biomolecular Engineering, Johns Hopkins University, 3400 North Charles Street, Baltimore, MD 212018, USA.
† Electronic Supplementary Information (ESI) available. See DOI: 10.1039/x0xx00000x

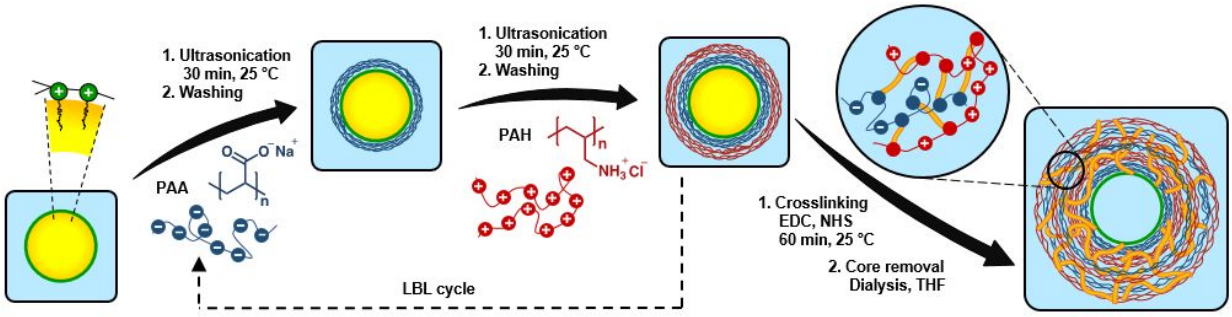

Scheme 1. LBL synthesis of crosslinked PEM NCs using crystallized miniemulsion NPs with covalently-stabilized surfactant layers as substrate.

With long-term research interest in polymeric NCs,[3d, 9] we have recently investigated LBL preparation of NCs using crystallized miniemulsion nanoparticles (NPs) as special sacrificial cores. As compared to typical emulsions, miniemulsions have significant kinetic stability.[10] Our previous studies demonstrated that crystallization of the dispersed oil phase leads to crystallized miniemulsion NPs with higher colloidal stability because of surface-anchored surfactant molecules.[9a, 9b] The dynamic stability of their surfactant monolayers on NPs' surface can be further enhanced through covalent stabilization. **Scheme 1** shows the general procedure for the preparation of the crystallized miniemulsion NPs. In brief, NPs were obtained by miniemulsification of a mixture consisting of *n*-docosane (dispersed phase; m.p. = 42-45 °C), water (continuous phase), and polymerizable surfactants at 50 °C, following by cooling to room temperature (r.t.) and subsequent UV-induced (λ_{max} = 365 nm) photo-crosslinking of surfactant monolayers. The crystallinity of the oil interior of the miniemulsion NPs at room temperature was verified by analysis using differential scanning calorimetry (DSC) prior to covalent stabilization of surfactant monolayers (**Fig. S1**). The dimension of these NPs can be adjusted through miniemulsion formulation, and specifically increases with oil amount (**Fig. S2**). The quaternary ammonium bromide functionality of the surfactants results in positive surface charge (~+60 mV) of the resulting narrowly-dispersed NPs (**Fig. S3**). Covalent-stabilization of the surfactant monolayers is critically important for increasing their dynamic stability and maintaining the colloidal stability of these NPs for LBL coating (**Scheme S1**). With the treatment of poly(acrylic acid) (PAA) in the form of sodium salt, the NPs stabilized by only small molecule surfactants formed aggregates, and this result was ascribed to the partial peeling off these surfactants from the surface of NPs due to their electrostatic interactions with PAA. However, NPs with crosslinked or polymerized surfactant monolayers were colloidal stable under the same conditions.

The synthesis of PEM NCs started with the preparation of PEM-coated NPs by LBL coating of PAA and poly(allylamine hydrochloride) (PAH) on crystallized miniemulsion NPs (**Scheme 2**), which have crosslinked surfactant monolayers and a volume-average hydrodynamic diameter ($D_{h,V}$) of 98 ± 1 nm (**Fig. S3**). PAA and PAH carry negative and positive charges because of their carboxylic salt and pronated amine moieties, respectively. They can form polycomplexes via electrostatic interactions.[11] PAA (M_W^{GPC} = 5.1 kDa) and PAH (M_W^{GPC} = 17.5 kDa) solutions were prepared in ultra-pure water at neutral pH with a concentration of 10 mM with respect to their monomer units. No additives were employed to adjust the pH of the polyelectrolyte solutions. The alternative LBL deposition of PAA and PAH was performed by adding their respective solutions to the solution of substrate NPs, followed by washing. In each coating process, excess amount of polyelectrolyte was used. The deposition process lasted for 30 min, with the assistance of mild ultrasonication to minimize aggregation of NPs at around isoelectric point. Because the resulting NPs have lower density than water, centrifuge dialysis technique (MWCO = 30 kDa) was used successfully to wash the coated NPs. The washed coated NPs showed ζ of ~-40 and +50 mV upon the deposition of PAA and PAH, respectively (**Fig. 1a**). The alternating positive and negative changes in ζ values upon the coating of a new PE layer

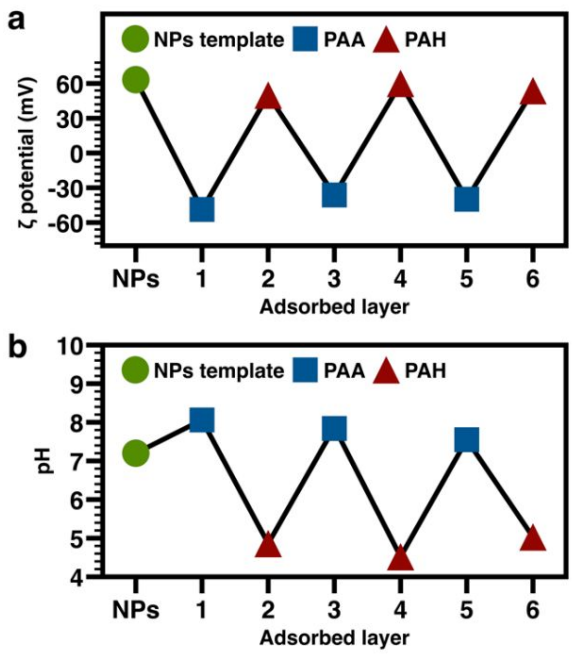

Fig. 1 a) Zeta potential of PEM-coated NPs as a function of PAA/PAH adsorbed layer number. b) pH of resultant solutions of NPs as a function of PAA/PAH adsorbed layer number.

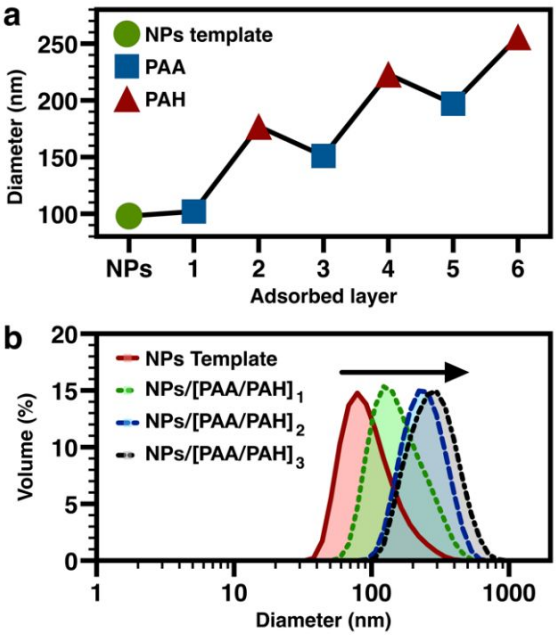

Fig. 2 a) $D_{h,V}$ measured by DLS as a function of number of PAA/PAH adsorbed layerson the crystallized miniemulsion NPs; b) Volume-average size distribution change for consecutive bilayer deposition on NPs. There arrow shows the direction of LBL cycle as the number of bilayers increase. Each dashed curve corresponds to a triangle data point in Fig 2a.

indicates the successful PE deposition through electrostatic adsorption. The relatively high absolute values of ζ are critical to maintain the colloidal stability of these NPs. Because both PAA and PAH are weak polyelectrolytes with pH-dependent ionization level,[12] pH variation of the solutions of NPs during LBL process was observed (**Fig. 1b**). Solutions of PAA-coated NPs retained slightly basic pH around 8 because the COO^- moieties can induce the generation of OH^-. On the other hand, solutions of PAH-coated NPs possessed acidic pH around 5 due to excess H^+ provided by the protonated amines of PAH.

The dimensions of the LBL NPs were characterized by dynamic light scattering (DLS). The change of $D_{h,V}$ of the NPs was revealed by DLS analysis (**Fig. 2**). With net results of continuous increase of $D_{h,V}$ of NPs upon each PAA/PAH deposition cycle, the increase in $D_{h,V}$ of NPs by PAH-coating was significant each time, but the subsequent PAA-coating resulted in slight shrinkage of $D_{h,V}$ values, presumably because PAA with relatively small molecular size could effectively condense the newly formed outer PAA/PAH complex bilayer. The DLS results also indicated absence of severe aggregation of NPs during the LBL process.[11]

Subsequently, crosslinked PEM NCs were obtained after chemical crosslinking the PEM of LBL NPs, followed by core removal. The purpose of chemical crosslinking is to covalently stabilize the PEM structures, which otherwise can be highly sensitive to environmental conditions and may readily undergo unfavorable aggregation or dissociation upon medium change. Following the approach reported by Caruso and co-workers,[11] amidation crosslinking was performed for PAA/PAH PEMs of the NPs (**Scheme S2**), in the presence of 1-ethyl-3-(3-dimethylaminopropyl)carbo-diimide (EDC) and *N*-hydroxysuccinimide (NHS). The successful crosslinking was

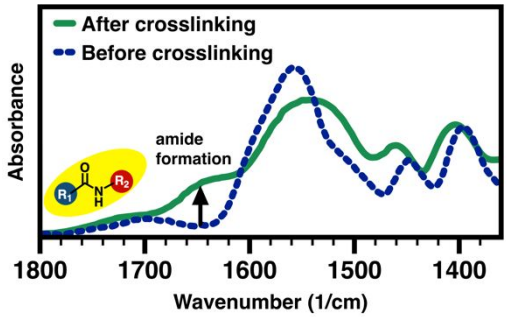

Fig. 3 FT-IR spectra of crosslinked $[PAA/PAH]_3$ NCs (solid line) and NPs/$[PAA/PAH]_3$ (dashed line). The arrow represents the formation of amide bond (with adsorption at 1650 cm^{-1}), occurred during crosslinking reaction between $–COO^-$ functionality of PAA and $–NH_3^+$ functionality of PAH, catalysed by EDC and NHS. R_1 and R_2 represent PAA and PAH backbone respectively.

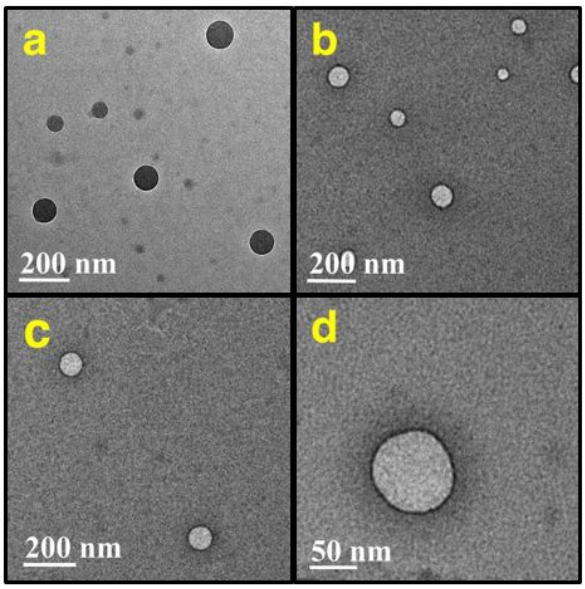

Fig. 4 a) TEM image of shell-crosslinked NPs/$[PAA/PAH]_3$ after shell crosslinking. b-d) TEM images of crosslinked $[PAA/PAH]_3$ NCs

verified by FT-IR analysis (**Fig. 3**), based on the appearance of amide C=O stretch adsorption at ~1650 cm^{-1} for the resulting PEM-crosslinked NPs as a result of amidation crosslinking. In addition, DLS monitoring of the crosslinking process also provide supporting evidence for the occurrence of amidation crosslinking by tracking the zeta potential change. With the occurrence of crosslinking reaction, the zeta potential value of the NPs decreased from +54 ± 2 mV to +34 ± 3 mV. Formation of amide crosslinking bonds between coated multilayers of PAA and PAH eliminated the charged functionalities and retained less ionized state, leading to the lower zeta potential value.

Well-defined NCs with crosslinked PEM shells were achieved by removal of crystallized *n*-docosane core of the LBL NPs. The core removal was readily performed by dialysis of the NPs against tetrahydrofuran (THF), which is a good solvent of docosane. The resulting crosslinked PEM NCs can be readily dispersed in water. Similarly, the NCs with non-crosslinked PEM shells were also prepared following the same procedure of core removal for NPs/$[PAA/PAH]_3$ without shell-crosslinking.

As compared with the shell-crosslinked NPs/$[PAA/PAH]_3$ templates ($D_{h,V}$ = 256 ± 4 nm; +34 ± 3 mV), the crosslinked NCs ($D_{h,V}$ = 235 ± 6 nm; ζ = +25 ± 3 mV) exhibited ~8% shrinkage in hydrodynamic size, due to the contraction of their network after the core removal (**Fig. S4**). DLS analysis also indicated that extent of size shrinkage increases considerably with the size of NCs. Because the NCs have the same PEM shell structures, such results further suggested that their physical strength and resistance to shrinkage decrease with the increase of the ratio of diameter to shell thickness.[13] DLS analysis demonstrated that the crosslinking of PEM shells led to NCs with robust structures that can stand for sonication treatment (**Figs. S5-S6**). As a comparison, the non-crosslinked NCs were more swollen and showed bigger hydrodynamic dimensions ($D_{h,V}$ = 343 ± 8 nm), but dissembled with the formation of aggregates after a mild sonication.[1b, 1c]

According to TEM imaging, the shell-crosslinked NPs/$[PAA/PAH]_3$ exhibited a dry-state surface average diameter (D_{av}) of 96 ± 12 nm, while the corresponding NCs showed a D_{av} of 87 ± 11 nm, with shell thickness of ~6 nm (**Figs. 4** and **S7**). The average thickness of only ~2 nm for each bilayer was ascribed to the relatively small molecular sizes of PAA and PAH used in this work.[11] Because these NCs have inner shell surface adsorbed with covalent-stabilized surfactant monolayers carrying hydrophobic tails, hydrophobic cargoes, such as nile red, can be readily encapsulated by their inner cavities (**Fig. S8**).

In summary, the LBL approach using crystallized miniemulsion NPs with covalently-stabilized surfactant layers as sacrificial templates has been demonstrated for the preparation of crosslinked PEM NCs. By using PAA/PAH as exemplary pair of polyelectrolytes with opposite charges, the resulting NCs showed well-defined capsular structures and well-controlled nanoscopic dimensions. Because these sacrificial NPs possess high colloidal stability and their crystallized oil phase can be readily removed by using organic solvent under mild synthetic conditions, this approach may allow to access a broad variety of well-defined NCs with different compositions.

This work was supported by U. S. National Science Foundation [CHE-1412785; CHE-1412985].

Conflicts of interest

There are no conflicts to declare.

References

1. (a) F. Caruso, R. A. Caruso and H. Möhwald, *Science*, 1998, **282**, 1111-1114; (b) J. Cui, M. P. v. Koeverden, M. Müllner, K. Kempe and F. Caruso, *Adv. Colloid Interface Sci.*, 2014, **207**, 14-31; (c) W. Tong, X. Song and C. Gao, *Chem. Soc. Rev.*, 2012, **41**, 6103-6124; (d) W. Meier, *Chem. Soc. Rev.*, 2000, **29**, 295-303; (e) A. P. Esser-Kahn, S. A. Odom, N. R. Sottos, S. R. White and J. S. Moore, *Macromolecules*, 2011, **44**, 5539-5553; (f) D. Y. Zhu, M. Z. Rong and M. Q. Zhang, *Prog. Polym. Sci.*, 2015, **49-50**, 175-220; (g) H. Sun, C. K. Chen, H. Cui and C. Cheng, *Polym. Int.*, 2016, **65**, 351-361; (h) K. C. Bentz and D. A. Savin, *Polym. Chem.*, 2018, **9**, 2059-2081.
2. (a) H. Sun, J. Cui, Y. Ju, X. Chen, E. H. H. Wong, J. Tran, G. G. Qiao and F. Caruso, *Bioconjugate Chem.*, 2017, **28**, 1859-1866; (b) X. Roy, J. K.-H. Hui, M. Rabnawaz, G. Liu and M. J. MacLachlan, *J. Am. Chem. Soc.*, 2011, **133**, 8420-8423.
3. (a) C. E. Mora-Huertas and H. E. Fessi, A., *Int. J. Pharm.*, 2010, **385**, 113-142; (b) S. De Koker, R. Hoogenboom and B. G. De Geest, *Chem. Soc. Rev.*, 2012, **41**, 2867-2884; (c) B. Miksa, *RSC Advances* 2015, **5**, 87781-87805; (d) C.-K. Chen, W.-C. Law, R. Aalinkeel, Y. Yu, B. Nair, J. Wu, S. Mahajan, J. L. Reynolds, Y. Li, C. K. Lai, E. S. Tzanakakis, S. A. Schwartz, P. N. Prasad and C. Cheng, *Nanoscale*, 2014, **6**, 1567-1572; (e) P. Yang, D. Li, S. Jin, J. Ding, J. Guo, W. Shi and C. Wang, *Biomaterials*, 2014, **35**, 2079-2088.
4. Y. Yan, M. Björnmalm and F. Caruso, *Chem. Mater.*, 2013, **26**, 452-460.
5. (a) D. O. Grigoriev, T. Bukreeva, H. Möhwald and D. G. Shchukin, *Langmuir*, 2008, **24**, 999-1004; (b) K. Szczepanowicz, H. J. Hoel, L. Szyk-Warszynska, E. Bielańska, A. M. Bouzga, G. Gaudernack, C. Simon and P. Warszynski, *Langmuir*, 2010, **26**, 12592-12597.
6. (a) E. Tjipto, K. D. Cadwell, J. F. Quinn, A. P. R. Johnston, N. L. Abbott and F. Caruso, *Nano Lett.*, 2006, 2243-2248; (b) C. Priest, A. Quinn, A. Postma, A. N. Zelikin, J. Ralston and F. Carusoo, *Lab Chip*, 2008, **8**, 2182-2187.
7. (a) W. C. Mak, K. Y. Cheung and D. Trau, *Chem. Mater.*, 2008, **20**, 5475-5484; (b) W. C. Mak, J. Bai, X. Y. Chang and D. Trau, *Langmuir*, 2009, **25**, 769-775.
8. (a) F. J. Rossier-Miranda, K. Schroën and R. Boom, *Langmuir*, 2010, **26**, 19106-19113; (b) T. Zeng, D. Yang, H. Li, C. Cheng and Y. Gao, *Polym. Chem.*, 2018, **9**, 627-636.
9. (a) Y. Li, E. Themistou, B. P. Das, L. Christian-Tabak, J. Zou, M. Tsianou and C. Cheng, *Chem. Commun.*, 2011, **47**, 11697-11699; (b) B. Sun, H. Sun, Y. Li, H. Cui and C. Cheng, *Eng. Sci.*, 2018, **5**, DOI: 10.30919/es30918d30536; (c) C. K. Chen, Q. Wang, C. H. Jones, Y. Yu, H. G. Zhang, W. C. Law, C. K. Lai, Q. H. Zeng, P. N. Prasad, B. A. Pfeifer and C. Cheng, *Langmuir*, 2014, **30**, 4111-4119; (d) Y. Li, L. Christian-Tabak, V. L. F. Fuan, J. Zou and C. Cheng, *J. Polym. Sci. A: Polym. Chem.*, 2014, **52**, 3250-3259.
10. K. Landfester, *Angew. Chem. Int. Ed.*, 2009, **48**, 4488-4507.
11. P. Schuetz and F. Caruso, *Adv. Funct. Mater.*, 2003, **13**, 929-937.
12. J. Choi and M. F. Rubner, *Macromolecules*, 2005, **38**, 116-124.
13. (a) T. Ohtsubo, S. Tsuda and K. Tsuji, *Polymer*, 1991, **32**, 2395-2399; (b) E. Pisani, N. Tsapis, B. Galaz, M. Santin, R. Berti, N. Taulier, E. Kurtisovski, O. Lucidarme, M. Ourevitch, B. T. Doan, J. C. Beloeil, B. Gillet, W. Urbach, S. L. Bridal and E. Fattal, *Adv. Funct. Mater.*, 2008, **18**, 2963-2971; (c) D. Lensen, E. C. Gelderblom, D. M. Vriezema, P. Marmottant, N. Verdonschot, M. Versluis, N. D. Jong and J. C. V. Hest, *Soft Matter*, 2011, **7**, 5417-5422.